J. Gen. Appl. Microbiol., **62**, 83–89 (2016)
doi 10.2323/jgam.62.83

jGAM

Full Paper

Exploration of a N-terminal disulfide bridge to improve the thermostability of a GH11 xylanase from *Aspergillus niger*

(Received October 1, 2015; Accepted November 30, 2015)

Chen-Yan Zhou,[1,*,#] Tong-Biao Li,[1,#] Yong-Tao Wang,[2] Xin-Shu Zhu,[1] and Jing Kang[1]

[1] *School of Life Science and Technology, Xinxiang Medical University, Jinsui Road, Xinxiang 453003, P.R. China*
[2] *The First Affiliated Hospital, Xinxiang Medical University, Jiankang Road, Weihui 453100, P.R. China*

To improve the thermostability of xylanase XynZF-2 from *Aspergillus niger* XZ-3S, a disulfide bridge was introduced in the N-terminal domains by site-directed mutagenesis (V1C and E27C). Simultaneously, the active sites of XynZF-2 were predicted by bioinformatics software and verified by site-directed mutagenesis (E103D and E194D). The mutated active sites *xynED*- and the mutated disulfide bridge *xynDC*-encoding genes were constructed and expressed in *Escherichia coli* BL21 (DE3). Compared to the native xylanase, it was found that the residual activity of the mutated XynED was 0.17%. The optimum temperature of the variant XynDC was increased to 45°C from 40°C of XynZF-2. After treatment at 40°C for 60 min, the variant XynDC retained 66.77% of their original activity, while the XynZF-2 retained about 44.36% residual activity. $t_{1/2}^{45^{\circ}C}$ of the variant XynDC also increased from 7 min to 14 min. The results of the mutated xylanases indicated that the active center of XynZF-2 mainly consisted of two catalytic residues (Glu103 and Glu194), and the introduction of a disulfide bridge in the N-terminal domains can improve the thermostability of XynZF-2.

Key Words: disulfide bridge; site-directed mutagenesis; thermostability; xylanase

Introduction

Xylanases (EC 3.2.1.8) are glycoside hydrolases that hydrolyze β-(1,4)-D-xylosidic linkages of xylans (Goswami et al., 2014; Zhang et al., 2014), which are one of most abundant hemicellulose hydrolases in nature and are found in fungi, bacteria, marine algae, crustaceans, etc. (Collin et al., 2005; Trevizano et al., 2012). Xylanases are mainly distributed in glycoside hydrolase (GH) families 11 and 10 (Li et al., 2015; Tan et al., 2014; Xue et al., 2012). The structure of GH family 10 xylanases consists mainly of a (β/α)8 barrel fold, which looks like a bowl (Wang et al., 2014). Compared with GH family 10 xylanases, GH family 11 xylanases possess idiosyncratic selectivity on substrates containing D-xylose and have simple protein domains, which is a general folding pattern composed of two β-sheets and one α-helix forming a partially-closed right-hand structure (Li et al., 2013; Song et al., 2014; Yin et al., 2014; Zhang et al., 2014).

Xylanases are vital industrial enzymes which are widely used in pulp bleaching, feed processing, biofuels and other areas of industry (Qian et al., 2015; Satyanarayana, 2013). Because of the low activity and thermostability of xylanases in general, the applicability of xylanases in industrial processes is restricted under high temperature conditions (Qian et al., 2015; Wang et al., 2012). In addition, thermophilic xylanases have many significant advantages in industrial applications, such as enhancing productivity and reducing energy consumption and environmental disruption (Collin et al., 2005; Liu et al., 2011). However, most wild-type xylanases belong to mesophilic xylanases, the structures of which are slightly different from thermophilic xylanases in local regions (Beg et al., 2001). Published studies have suggested that N-terminus, C-terminus and α-helix domains of xylanase are critical for its thermostability (Yin et al., 2013b; You et al., 2010). It has also been confirmed that the thermostability of xylanases can be influenced by the introduction of salt bridge, disulfide bridge, hydrogen bond and aromatic

*Corresponding author: Chen-Yan Zhou, School of Life Science and Technology, Xinxiang Medical University, Jinsui Road, Xinxiang 453003, P.R. China.
Tel: +86-373-3831677 Fax: +86-373-3029887 E-mail: zhouchenyan2008@163.com
#These authors contributed equally to this work.

None of the authors of this manuscript has any financial or personal relationship with other people or organizations that could inappropriately influence their work.

amino acid substitutions (Fenel et al., 2004; Tan et al., 2014; Wang et al., 2012; Yin et al., 2014). Of these, the disulfide bridge has attracted much attention.

In our previous work, the xylanase (XynZF-2) gene (Genbank code: JQ7000382) was cloned from *Aspergillus niger* (Fu et al., 2012). The xylanase XynZF-2 belongs to the mesophilic GH11 xylanases, and the measured optimum temperature was 40°C, which verified that XynZF-2 had poor thermostability. This study was mainly focused on improving the thermostability of XynZF-2, and primarily consisted of two parts. Firstly, the active sites of XynZF-2 were analyzed to avoid the introduction of amino acid residues on thermostability reducing the activity of XynZF-2. Secondly, a disulfidge bridge at N-terminal domains was introduced to improve the thermostability of XynZF-2. In addition, all of the mutated genes were artificially synthesized with synonymous codons biasing towards *Escherichia coli*, and expressed into *Escherichia coli* BL21 (DE3).

Materials and Methods

Materials. *Aspergillus niger* XZ-3S strain was preserved in our laboratory. The plasmid pET-28a and *Escherichia coli* BL21 (DE3) were purchased from Novagen (USA). The recombinant pET-28a-*xynZF*-2 was constructed and preserved in our laboratory. Taq polymerase, Pyrobest DNA polymerase, T4 DNA ligase, restriction enzymes, X-gal and IPTG were purchased from TaKaRa (Dalian, China). Ampicillin, a UNIQ-10 column DNA gel extraction kit and Kanamycin were purchased from Sangon (Shanghai, China). The HiTrap affinity column for Ni^{2+}-chelating chromatography was purchased from Amersham Pharmacia Biotech (Sweden). *Escherichia coli* BL21 (DE3) was cultivated in Luria-Bertani (LB) medium (5 g L^{-1} yeast extract, 10 g L^{-1} peptone, and 10 g L^{-1} NaCl).

Analysis and computer modeling of the xylanase structures. The ProtParam program was used to analyze the physicochemical properties of xylanases (http://web.expasy.org/protparam/). The homology sequence and the 3D structure of the xylanases were determined using the phyre2 (http://www.sbg.bio.ic.ac.uk/phyre2/html/page.cgi?id=index). The 3D structure of the xylanases were viewed and analyzed by DS ViewerPro6.0. The disulfide bridge was predicted by the DiANNA 1.1 web server (http://bioinformatics.bc.edu/clotelab/DiANNA/) (Yin et al., 2013b). The active center of the xylanases was predicted by PROSITE (http://prosite.expasy.org) (Jeong et al., 2007).

Site-directed mutagenesis and construction of the recombinant vector. Using pET-28a-*xynZF*-2 as the template, the mutant genes *xynED* and *xynDC* were amplified with the method of overlap extension PCR (Chen et al., 2010), which was accomplished with the primers listed in Table 1. The amplified conditions were as follows: 94°C for 2 min; 30 cycles of 94°C for 30 s, 55°C for 30 s, 72°C for 1 min; and an elongation at 72°C for 10 min. The mutant genes *xynED* and *xynDC* were inserted, respectively, into pET-28a, followed by transforming them into *Escherichia coli* BL21 (DE3). The resulting recombinant *Escherichia coli* BL21/pET-28a-*xynED* and BL21/pET-28a-*xynDC* were screened on LB medium including 100 μg/mL kanamycin. The respective transformants were confirmed by DNA sequencing.

Table 1. The names and sequences of the mutated primers.

Primer name	Primer sequence (5′-3′)
225-BC	CCGGAATTCGTTCCCCACGACTCTGTCG (*Eco*R′ site)
225-BZ	CCCAAGCTTTTACTGAACAGTGATGGACG (*Hind*′ site)
E103D-F	CCTGATCGATTACTACATCGTC
E103D-R	CTCGACGATGTAGTAATCGATC
E194D-R	GATGGACGAAGATCCACTGCTCTGGTAACCATCG
V1C-F	CCGGAATTCTGTCCCCACGACTCTGT (*Eco*R′ site)
E27C-F	CGGCTGTAACAACGGCTTCTA
E27C-R	GGAGTAGTAGAAGCCGTTGTTACAGCC

The mutant codons are underlined, and the restriction enzyme sites are boxed.

Expression and purification of the variant xylanases. The transformants, cultured at 37°C overnight, were diluted 1/50 in LB medium including 100 μg/mL kanamycin. The seed cultures were shaken at 230 rpm and incubated at 37°C until A_{600} reached 0.6, and then the cultures were induced with isopropyl-β-D-thiogalactopyranoside (IPTG, 2 mM) and incubated at 37°C for 2 h (Fu et al., 2012; Qian et al., 2015). The cells were collected by centrifugation at 8000 rpm for 15 min. In addition, *Escherichia coli* BL21 with pET-28a was induced and expressed as a control. Then the cells were resuspended by Na_2HPO_4-citric acid buffer (pH 4.6) and were lysed by ultrasonic treatment. Supernatants were harvested by centrifugation at 8000 rpm for 20 min at 4°C. The mutant xylanase XynDC and the wildtype XynZF-2 were purified by ProteinPure Ni-NTA Resin, according to the manufacturer's instructions. The purified enzymes were analyzed by 12% SDS-PAGE. For visualizing the protein bands, the polyacrylamide gel was stained by coomassie brilliant blue R-250 (Fu et al., 2012).

Enzyme assay. Xylanase activity was assayed by estimating the amount of reducing sugars liberated from 0.5% birchwood xylan, using a 3,5-dinitrosalicylic acid method (Li et al., 2013; Sriprang et al., 2006; Yin et al., 2013a, 2014). The reducing sugars were liberated by incubating 1 mL 0.5% birchwood xylan (in 50 mM Na_2HPO_4-citric acid buffer, pH 4.6) with 1.5 mL xylanase for 15 min at 40°C. One unit of enzyme activity was defined as the amount of enzyme releasing 1 μmol of xylose equivalent from birchwood xylan per minute under the assay conditions described above.

Enzyme properties. The optimum temperatures (XynED and XynDC) were estimated to be 35°C and 60°C by a 3,5-dinitrosali cylic acid method, respectively (Fu et al., 2012; Satyanarayana, 2013; Xue et al., 2012). The temperature at which the xylanase maintained the highest residual activity was defined to be the optimum temperature. To measure the thermostability of the variant xylanases, they were incubated at 40°C and 45°C, respectively, for 60 min in the absence of a substrate (Fu et al., 2012; Song et al., 2014; Yin et al., 2014). The

thermostability of the xylanases in this study was defined as the temperature at or below which the residual enzyme activity was reserved. The activity of the xylanases was estimated under standard assay conditions.

The optimum pH of the variant xylanases was evaluated over the pH range of 3.0–9.0 at the optimum temperature (Xue et al., 2012). The pH value at which the xylanase maintained the highest residual activity was defined to be the optimum pH. To determine the pH stability of the variant xylanases, the purified xylanases were incubated with various pH buffers at 40°C for 60 min. In addition, the various pH buffers were as follows: Na_2HPO_4-citric acid buffer (pH 3.0–5.0), Na_2HPO_4-NaH_2PO_4 buffer (pH 6.0–7.0), Tris-HCl buffer (pH 8.0) and glycin-NaOH buffer (pH 9.0). The control, which was not subjected to preincubation, was placed in ice. The effect of the various pH buffers on the residual activity of the variant xylanases were measured under standard assay conditions.

Results

Computer modeling and analysis of the xylanases

The prediction of the active sites indicated that two amino acid residues, Glu-103 and Glu-194 of XynZF-2, were located at the active center. The homology primary structure of XynZF-2 displayed identities of XynZF-2 with three other GH family 11 xylanases from *Penicillium funiculosum* (PDB code:d1te1b), *Escherichia coli* (PDB code:c2vu1A), and *Trichoderma harzianum* (PDB code:d1xnda), were 68%, 64% and 63%, respectively. Based on the above homology alignment of primary structures, the three-dimensional structure of XynZF-2 was modeled (Fig. 1a). This revealed that the three-dimensional structure of XynZF-2 conformed to the structure of GH family 11 xylanases composed of two β-sheets and one α-helix forming a partially-closed right-hand structure. The analysis of the XynZF-2 structure revealed that at the N-terminal domains a disulfide bridge could be introduced between position 1 and 27. The three-dimensional structure of a disulfide bridge mutation, XynDC, was modeled, which was similar to that of XynZF-2 (Fig. 1b). In addition, the designed disulfide bridge sites were far from the active center, which might indicate that the disulfide bridge mutation cannot reduce the xylanase activity.

Construction of the variant genes xynED and xynDC

The mutated gene *xynED* was constructed by substituting Glu-103 and Glu-194 with Asp. To construct the disulfide bridge mutation xylanase, *xynDC*, cysteines were introduced to position 1 and 27 at N-terminal regions (amino acid substitution V1C and E27C). Two approximately 620-bp bands of *xynED* and *xynDC* genes were amplified with sense and anti-sense primers (data not shown), which contained *Eco*R I and *Hin*d III restriction enzyme sites, respectively. The *xynED* and *xynDC* genes were inserted into vector pET-28a, and were then digested by *Eco*R I and *Hin*d III, respectively. The recombinant expression plasmids, pET-28a-*xynED* and pET-28a-*xynDC*, were then constructed and transformed into *Escherichia coli* BL21 (DE3). DNA sequencing results demonstrated that the cloned mutant *xynED* and *xynDC* were exactly 621 bp in length, as designed theoretically. Both of the mutant *xynED* and *xynDC* genes encoded 207-aa, which were similar to that of *xynZF*-2.

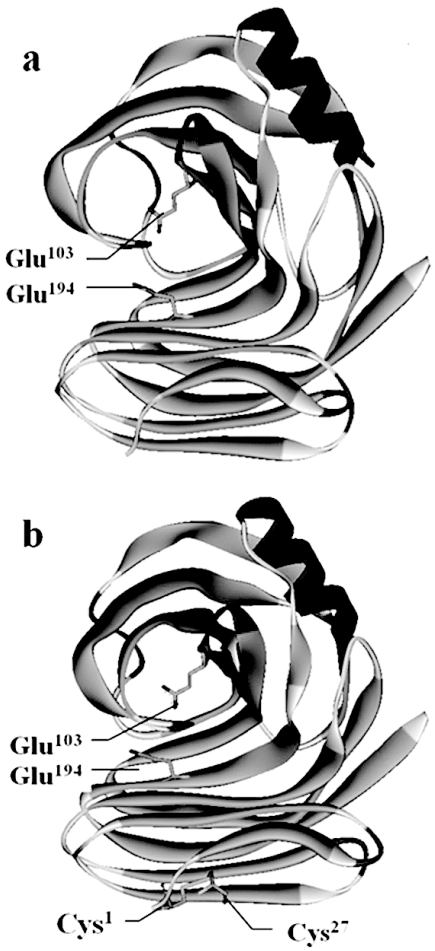

Fig. 1. Homology modeling of the xylanase 3-D structures.

(a) The 3-D structure of the native xylanase XynZF-2. Two catalytic residues, Glu103 and Glu194, are located at the active center. (b) The 3-D structure of the mutant xylanase XynDC. A disulfide bridge (Cys^1–Cys^{27}) was introduced into XynDC at N-terminal domains.

Expression of the variant gene xynED

The recombinant transformants, BL21/pET-28a-*xynED* and BL21/pET-28a-*xynZF*-2, were expressed with IPTG, and analyzed by SDS-PAGE. The recombinant transformant, BL21/pET-28a, was induced by IPTG as control. SDS-PAGE showed that cell extracts from the recombinant transformant BL21/pET-28a-*xynED* exhibited a clear band with a molecular weight of about 31 kDa, which was similar to XynZF-2 (Fig. 2). Because of the presence of the His-tag fusion peptide in expression vector pET-28a, the recombinant protein had 36 extra amino acids. For the foregoing reasons, the molecular weight of recombinant xylanases expressed in *E. coli* BL21 (DE3) were higher than the calculated molecular weight (24.04 kDa) (Fu et al., 2012). No band was observed in the extract from the non-induced BL21/pET-28a-*xynED* and the control strain BL21/pET-28a. The activity of the mutant XynED was 0.17% of the XynZF-2. It proved that glutamic

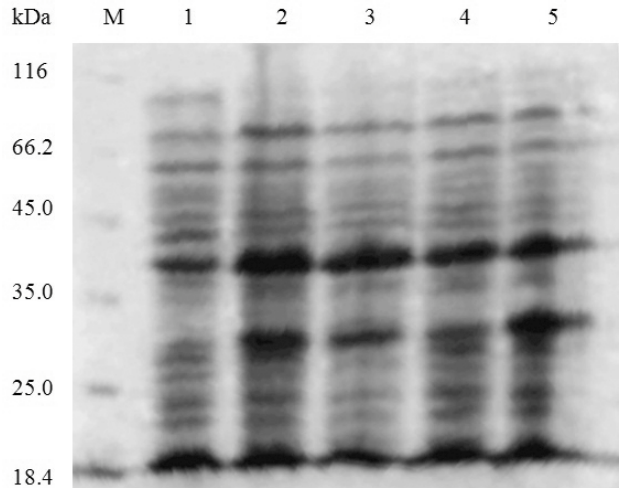

Fig. 2. SDS-PAGE analysis of the recombinant xylanases.

Lane M: protein markers; Lane 1: *E. coli* pET-28a with IPTG induction; Lane 2: *E. coli* pET-28a-*xynED* with IPTG induction; Lane 3: *E. coli* pET-28a-*xynED* without IPTG induction; Lane 4: *E. coli* pET-28a-*xynZF*-2 without IPTG induction; Lane 5: *E. coli* pET-28a-*xynZF*-2 with IPTG induction.

acid residues on the positions 103 and 194 were critical for the active center of XynZF-2.

Expression and purification of the variant XynDC

The *E. coli* pET-28a-*xynDC* and *E. coli* pET-28a-*xynZF*-2 were induced and expressed under the same conditions. The advantage of the pET-28a vector expression system was that it included a His-tag fusion peptide, which was fused into the N-terminal of the xylanase gene. Therefore, xylanases expressed in the pET-28a vector could be purified using Ni^{2+} affinity chromatography. SDS-PAGE analysis demonstrated that the molecular weight of purified XynDC was 31 kDa, which was consistent with the purified XynZF-2 (Fig. 3) (Fu et al., 2012).

Characterization of the recombinant xylanase XynDC

The optimum temperature of the mutated XynDC, measured at pH 4.6 for 15 min, was 45°C, which was 5°C higher than that of the recombinant xylanase XynZF-2 (Fig. 4). Indeed, the mutant containing disulfide bridges will be less flexible. The flexibility correlated directly with the enzymatic activity, which explains why, at 35°C, the enzyme activity of XynDC was just only 50% of the enzyme activity of XynZF-2. To estimate the thermostability, the residual activities of the recombinant xylanases were measured after incubation at different temperatures for 60 min. After incubation at 40°C for 60 min, the residual activity of the recombinant XynZF-2 decreased to 44.36%, while the mutated XynDC maintained 66.77% residual activities. The thermal inactivation half-life of the XynZF-2 at 45°C was 7 min, while that of the mutated XynDC was 14 min. Moreover, the residual activity of the XynZF-2 declined rapidly, and disappeared after incubation at 45°C for 20 min. In contrast, the activity of the XynDC declined slowly under the same conditions, and 37.54% of the residual activity was reserved after incubation at 45°C for 20 min (Fig. 5). These results verified that the introduction of a disulfide bridge at N-terminal domains had a positive effect on the thermotolerance of XynZF-2.

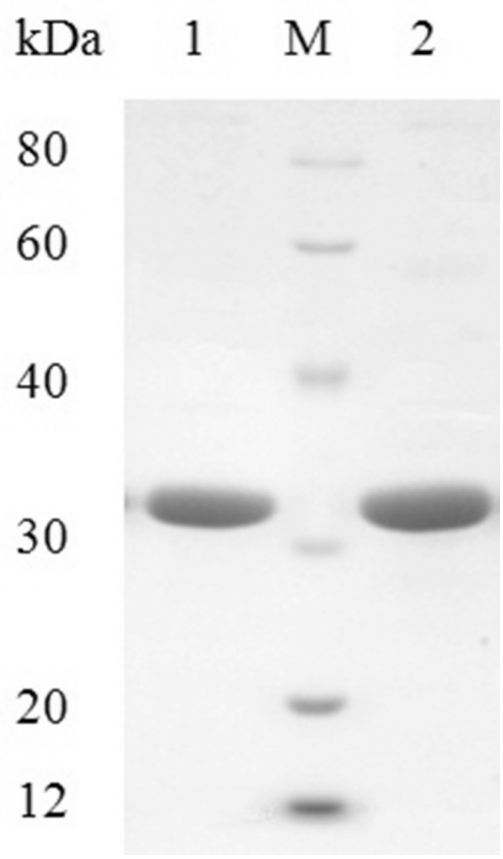

Fig. 3. SDS-PAGE analysis of the recombinant xylanase XynDC.

Lane M: protein markers; Lane 1: purified XynZF-2; Lane 2: purified XynDC.

The optimum pH of the mutated XynDC was pH 5.0 which was the same as that of XynZF-2 (Fig. 6). Although the optimum pHs were similar, the pH stabilities of the mutated XynDC and XynZF-2 were different. At 40°C for 60 min, XynDC maintained more than 50% activity between pH 3.0 and pH 9.0 which was broader than that of XynZF-2 (Fig. 7).

Discussion

The thermal stability of GH family 11 xylanases has been studied extensively by a variety of methods (Bankeeree et al., 2014; Ding and Cai, 2013; Hakulinen et al., 2003; Paës and O'Donohue, 2006; Xie et al., 2011). Nevertheless, there are two principal approaches used to obtain the thermotolerance xylanases. Firstly, the mesophilic and high specific activity xylanases were transformed into thermophilic xylanases by molecular modification. Secondly, the natural thermophilic xylanases were sifted from the thermophilic microorganism (Verma and Satyanarayana, 2012).

The C-terminus of GH family 11 xylanases is buried in the β-sheets, while the N-terminus is located on the fringe of β-sheets and contact to the hydrophilic environment. This indicated that the N-terminus of GH family 11 xylanase was more easily unfolded than the C-terminus (Li et al., 2012). An advance in the thermostability of xylanase AuXyn11A from *Aspergillus usamii* E001 has

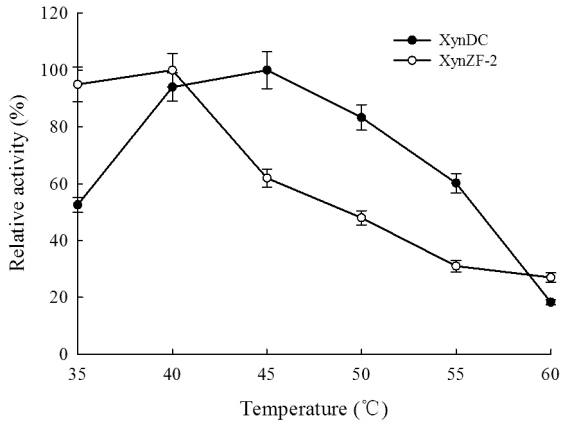

Fig. 4. Effect of temperature on the activities of XynDC and XynZF-2.

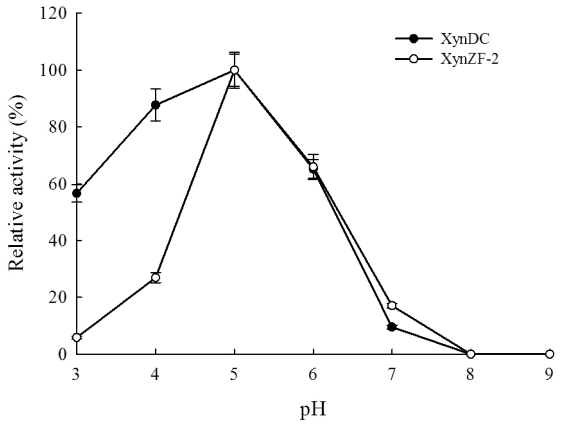

Fig. 6. Effect of pH on the activities of XynDC and XynZF-2.

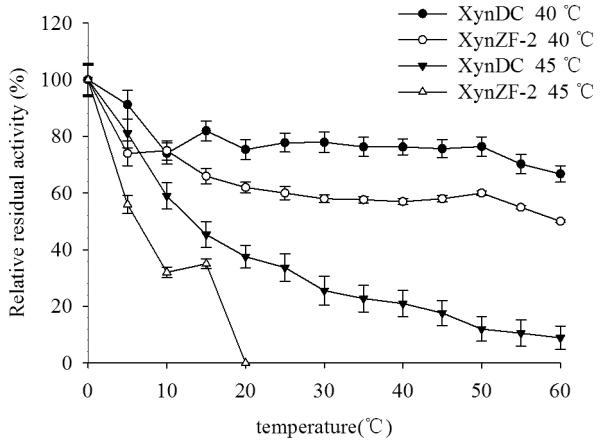

Fig. 5. Effect of temperature on the stabilities of XynDC and XynZF-2.

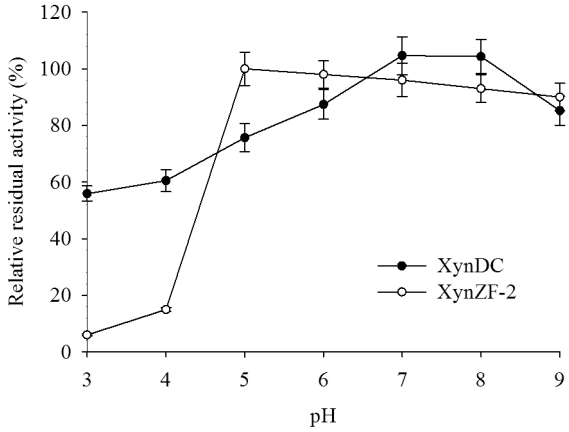

Fig. 7. Effect of pH on the stabilities of XynDC and XynZF-2.

been reported by Zhang et al. (2014). They substituted the N-terminal 33 amino acids of AuXyn11A into the corresponding 38 amino acids of *Ev*Xyn11^{TS}, which consequently obtained a high thermostability, and also the optimum temperature of the mutated AEXynM was increased by 20°C over AuXyn11A, which demonstrated that the substituted N-terminus had a significant effect on the thermostability of AuXyn11A. It has also been reported that the deletion of N-terminal sequence of Xyn11 from the filamentous fungus *Bispora antennata* decreased its thermostability (Liu et al., 2015). In conclusion, the xylanase N-terminus is an important region regarding thermostability, of stabilization extremely improves the entire thermostability of the GH family 11 xylanases (Yin et al., 2014).

In addition, site-directed mutagenesis has a significant effect on the thermostability of xylanases, which is also well known (Chen et al., 2010). However, there is a risk that the activity of xylanases could decrease, when the mutated sites on thermostability are located close to the active site canyon (Li and Turunen, 2014). In this study, in order to avoid site-directed mutagenesis on thermostability affecting the active site canyon, the active sites of xylanase XynZF-2 were predicted by PROSITE and verified by site-directed mutagenesis (E103D and E194D).

It is well known that a single amino acid substitution can have a remarkable effect on enzyme thermostability, so it would be difficult to compare the sequence of mutation sites of different xylanases from previous studies, and it might also be impossible to reveal credible regularity to guide site-directed mutations of GH family 11 xylanase on the basis of the results of a comparison (Xue et al., 2012). Though the sequences of GH family 11 xylanases are various, the 3D structures are similar. Therefore, in this study, a disulfide bridge was introduced into the 3D structure of XynZF-2 from a comparison of previous studies (Li et al., 2013). A thermostable mutant, XynDC, was obtained and included two amino acid substitutions, V1C and E27C, which were located at the N-terminal domains. Compared with XynZF-2, XynDC showed an increase in optimum temperature of 5°C. At 40°C, XynZF-2 maintained a 44.36% residual activity after incubation at 40°C for 60 min without the substrate, but the mutated XynDC maintained a 66.77% residual activity. At 45°C, the thermal inactivation half-life of XynDC was improved by 7 min.

In conclusion, these results verified that improving the

thermostability of xylanase XynZF-2 from *Aspergillus niger* can be accomplished via the introduction of a disulfide bridge at N-terminal regions. Since many thermophilic GH family 11 xylanases contain disulfide bridges, it is likely that the largest number of disulfide bridges may play a vital role in protein folding and stability. In addition, many disulfide bridges are closely associated with the thermostability of protein, and enhancing the stability of the protein structure is accomplished through reducing the entropy of the protein unfolding state. As a consequence, the disulfide bridge mutation of XynZF-2 at N-terminal regions reduced the unfolding state and strengthened the N-terminal stability, which stabilized the overall xylanase structure and improved the thermostability of XynZF-2.

To date, *P. pastoris* and *E. coli* are the most common expression systems used in industrial enzyme production. In general, *E. coli* expression systems have a high purification cost for recombinant proteins and complicated downstream processing, while *P. pastoris* expression systems secrete recombinant proteins into the medium and have a simple purification process. Meanwhile, *P. pastoris* produced many post-translation modifications (Chen et al., 2010). For instance, protein glycosylation, which regulates protein folding and turnover, plays a crucial role in the improvement of enzyme thermostability and activity (Raquel et al., 2013). In order to make further improvement on the thermostability of the disulfide bridge mutation XynDC, the *xynDC* gene will be expressed in *P. pastoris* in further research.

Acknowledgments

This study was financially supported by the Foundation of He'nan Educational Committee (No. 13A180861; 14A180018); the Foundation of He'nan Province of China for Key Young Teachers in University (No. 2011GGJS-125) and the Scientific Research Fund of Xinxiang Medical University (No. 2013ZD113).

References

Bankeeree, W., Lotrakul, P., Prasongsuk, S., Chaiareekij, S., Eveleigh, D. E. et al. (2014) Effect of polyols on thermostability of xylanase from a tropical isolate of *Aureobasidium pullulans* and its application in prebleaching of rice straw pulp. *Springer Plus*, **3**, 1–11.

Beg, Q., Kapoor, M., Mahajan, L., and Hoondal, G. (2001) Microbial xylanases and their industrial applications: a review. *Appl. Microbiol. Biotecnol.*, **56**, 326–338.

Chen, X. Z., Xu, S. Q., Zhu, M. S., Cui, L. S., Zhu, H. et al. (2010) Site-directed mutagenesis of an *Aspergillus niger* xylanase B and its expression, purification and enzymatic characterization in *Pichia pastoris*. *Process Biochem.*, **45**, 75–80.

Collin, T., Gerday, C., and Feller, G. (2005) Xylanase, xylanase families and extremophilic xylanases. *FEMS Microbiol. Rev.*, **29**, 32–23.

Ding, Y. R. and Cai, Y. J. (2013) Conformational dynamics of xylanase a from *Streptomyces lividans*: Implications for TIM-barrel enzyme thermostability. *Biopolymers*, **99**, 594–604.

Fenel, F., Leisola, M., Jänis, J., and Turunen, O. (2004) A de novo designed N-terminal disulphide bridge stabilizes the *Trichoderma reesei* endo-1,4-beta-xylanase II. *J. Biotechnol.*, **108**, 137–143.

Fu, G. H., Wang, Y. T., Wang, D. D., and Zhou, C. Y. (2012) Cloning, expression, and characterization of an GH11 xylanase from *Aspergillus niger* XZ-3S. *Indian. J. Microbiol.*, **52**, 682–688.

Goswami, G. K., Krishnamohan, M., Nain, V., Aggarwal, C., and Ramesh, B. (2014) Cloning and heterologous expression of cellulose free thermostable xylanase from *Bacillus brevis*. *Springer Plus*, **3**, 2–6.

Hakulinen, N., Turunen, O., Jänis, J., and Leisola, M. (2003) Three-dimensional structures of thermophilic b-1,4-xylanases from *Chaetomium thermophilum* and *Nonomuraea flexuosa* comparison of twelve xylanases in relation to their thermal stability. *Eur. J. Biochem.*, **270**, 1399–1412.

Jeong, M. Y., Kim, S., Yun, C. W., Choi, Y. J., and Cho, S. G. (2007) Engineering a de novo internal disulfide bridge to improve the thermal stability of xylanase from *Bacillus stearothermophilus* No. 236. *J. Biotechnol.*, **127**, 300–309.

Li, H. and Turunen, O. (2014) Effect of acidic amino acids engineered into the active site cleft of *Thermopolyspora flexuosa* GH11 xylanase. *Biotechnol. Appl. Biochem.*, **4**, 1–8.

Li, H., Murtomäki, L., Leisola, M., and Turunen, O. (2012) The effect of thermostabilising mutations on the pressure stability of *Trichoderma reesei* GH11 xylanase. *Protein Eng. Des. Sel.*, **25**, 821–826.

Li, H., Kankaanpää, A., Xiong, H. R., Hummel, M., Sixta, H. et al. (2013) Thermostabilization of extremophilic *Dictyoglomus thermophilum* GH11 xylanase by an N-terminal disulfide bridge and the effect of ionic liquid [emim] OAc on the enzymatic performance. *Enzyme Microbiol. Technol.*, **53**, 414–419.

Li, H., Voutilainen, S., Ojamo, H., and Turunen, O. (2015) Stability and activity of *Dictyoglomus thermophilum* GH11 xylanase and its disulphide mutant at high pressure and temperature. *Enzyme Microbiol. Technol.*, **70**, 66–71.

Liu, L. W., Zhang, G. Q., Zhang, Z., Wang, S. Y., and Chen, H. G. (2011) Terminal amino acids disturb xylanase thermostability and activity. *J. Biol. Chem.*, **286**, 44710–44715.

Liu, Q., Wang, Y. R., Luo, H. Y., Wang, L. W., Shi, P. J. et al. (2015) Isolation of a novel cold-active family 11 Xylanase from the *Filamentous Fungus Bispora antennata* and deletion of its N-terminal amino acids on thermostability. *Appl. Biochem. Biotechnol.*, **175**, 925–936.

Paës, G. and O'Donohue, M. J. (2006) Engineering increased thermostability in the thermostable GH-11 xylanase from *Thermobacillus xylanilyticus*. *J. Biotechnol.*, **125**, 338–350.

Qian, C. L., Liu, N., Yan, X., Wang, Q., Zhou, Z. H. et al. (2015) Engineering a high-performance, metagenomic-derived novel xylanase with improved soluble protein yield and thermostability. *Enzyme Microbiol. Technol.*, **70**, 35–41.

Raquel, F. M., Vieira, D. S., Alponti, J. S., Bonneil, E., Thibault, P. et al. (2013) Engineering the pattern of protein glycosylation modulates the thermostability of a GH11 xylanase. *J. Biol. Chem.*, **288**, 25522–25534.

Satyanarayana, D. V. T. (2013) Thermostabilization of extremophilic *Dictyoglomus thermophilum* GH11 xylanase by an N-terminal disulfide bridge and the effect of ionic liquid [emim] OAc on the enzymatic performance. *J. Microbiol. Biotechnol.*, **40**, 1373–1381.

Song, L. T., Dumon, C., Siguier, B., André, I., Eneyskaya, E. et al. (2014) Impact of an N-terminal extension on the stability and activity of the GH11 xylanase from *Thermobacillus xylanilyticus*. *J. Biotechnol.*, **174**, 64–72.

Sriprang, R., Asano, K., Gobsuk, J., Tanapongpipat, S., Champreda, V. et al. (2006) Improvement of thermostability of fungal xylanase by using site-directed mutagenesis. *J. Biotechnol.*, **126**, 454–462.

Tan, Z. B., Tang, C. D., Wu, M. C., He, Y., Hu, D. et al. (2014) Exploration of disulfide bridge and N-glycosylation contributing to high thermostability of a hybrid xylanase. *Protein Peptide Lett.*, **21**, 657–662.

Trevizano, L. M., Ventorim, R. Z., Rezende, S. T., Junior, F. P. S., and Guimarães, V. M. (2012) Thermostability improvement of *Orpinomyces* sp. xylanase by directed evolution. *J. Mol. Catal. B-Enzym.*, **81**, 12–18.

Verma, D. and Satyanarayana, T. (2012) Molecular approaches for ameliorating microbial xylanases. *Bioresource Technol.*, **117**, 360–367.

Wang, J. Q., Tan, Z. B., Wu, M. C., Li, J. F., and Wu, J. (2014) Improving the thermostability of a mesophilic family 10 xylanase, AuXyn10A, from *Aspergillus usamii* by in silico design. *J. Ind. Microbiol. Biotechnol.*, **41**, 1217–1225.

Wang, Y. W., Fu, Z., Huang, H. Q., Zhang, H. S., Yao, B. et al. (2012) Improved thermal performance of *Thermomyces lanuginosus* GH11 xylanase by engineering of an N-terminal disulfide bridge. *Bioresource. Technol.*, **112**, 275–279.

Xie, J., Song, L. L., Li, X. R., Yi, X. L., Xu, H. et al. (2011) Site-directed mutagenesis and thermostability of xylanase XYNB from *Aspergillus niger* 400264. *Curr. Microbiol*., **62**, 242–248.

Xue, H. P., Zhou, J. G., You, C., Huang, Q., and Lu, H. (2012) Amino acid substitutions in the N-terminus, cord and α-helix domains improved the thermostability of a family 11 xylanase XynR8. *J. Ind. Microbiol. Biotechnol*., **39**, 1279–1288.

Yin, X., Gong, Y. Y., Wang, J. Q., Tang, C. D., and Wu, M. C. (2013a) Cloning and expression of a family 10 xylanase gene (*Aoxyn10*) from *Aspergillus oryzae* in *Pichia pastoris*. *J. Gen. Appl. Microbiol*., **59**, 405–415.

Yin, X., Li, J. F., Wang, J. Q., Tang, C. D., and Wu, M. C. (2013b) Enhanced thermostability of a mesophilic xylanase by N-terminal replacement designed by molecular dynamics simulation. *J. Sci. Food Agr*., **93**, 3016–3023.

Yin, X., Yao, Y., Wu, M. C., Zhu, T. D., Zeng, Y. et al. (2014) A unique disulfide bridge of the thermophilic xylanase SyXyn11 plays a key role in its thermostability. *Biochemistry (Moscow)*, **79**, 531–537.

You, C., Huang, Q., Xue, H. P., Xu, Y., and Lu, H. (2010) Potential hydrophobic interaction between two cysteines in interior hydrophobic region improves thermostability of a family 11 xylanase from *Neocallimastix patriciarum*. *Biotechnol. Bioeng*., **105**, 861–871.

Zhang, H. M., Li, J. F., Wang, J. Q., Yang, Y. J., and Wu, M. C. (2014) Determinants for the improved thermostability of a mesophilic family 11 xylanase predicted by computational methods. *Biotechnol. Biofuels*, **7**, 1–10.